

A New Chloro-Bridged Cu^{II} Schiff Base Complex with Ferromagnetic Exchange Interaction

Shu-Lan Ma,^[a] Xu-Xia Sun,^[a] Song Gao,^[b] Chuan-Min Qi,^{*,[a]} Hai-Bo Huang,^[a] and Wen-Xiang Zhu^[a]

Keywords: Copper / Schiff bases / Dinuclear complex / Crystal structure / Magnetic properties

The synthesis and characterization of the μ -Cl-bridged dinuclear complex $[\text{CuLCl}]_2$ with the new Schiff-base ligand HL, 2-methyl-6-[(pyridine-2-ylmethylene)amino]phenol, is reported. The structural study shows the complex has the unusual distorted trigonal-bipyramidal geometry. Variable temperature susceptibility measurements in the range of 2.0–300 K reveal a novel ferromagnetic coupling, $2J = 1.52 \text{ cm}^{-1}$.

A comparison for the magnetic coupling of $[\text{CuLCl}]_2$ with other reported $\text{Cu}(\mu\text{-Cl})_2\text{Cu}$ compounds with square-pyramidal or trigonal-bipyramidal geometry is discussed in detail. The complex may provide useful information for the magneto-structural correlations of these compounds.

(© Wiley-VCH Verlag GmbH & Co. KGaA, 69451 Weinheim, Germany, 2007)

Introduction

Recently, chemists as well as physicists have concentrated their efforts on the study of multinuclear molecular-based magnetic materials so as to understand the magnetic interactions between the paramagnetic metal ions and the bridging ligands to develop the magneto-structural correlations enabling the design of interesting magnetic materials.^[1] The exchange coupling between the spins of unpaired electrons on metal atoms in polynuclear compounds is termed ferro- or antiferromagnetism, depending upon whether the individual spins in the ground state show a parallel or antiparallel alignment. The construction of molecular-based magnetic materials with ferromagnetic ordering is a major challenge. The relative simplicity of dinuclear systems has permitted the proposal of some magneto-structural correlations that are very useful for predicting magnetic properties of new compounds.

A good degree of success has been accomplished in correlating structure and magnetic properties for dihydroxo-bridged dinuclear copper complexes,^[2] but no unique magneto-structural correlation has been found for dichloro-bridged dinuclear copper complexes. Different magnetic behavior has been found in these systems and great difficulties remain in establishing a magneto-structural correlation due

to the much larger structural variety.^[3] Further investigations into the magneto-structural correlation of dichloro-bridged Cu^{II} dimers seem necessary.

We synthesize the tridentate Schiff-base ligand HL {2-methyl-6-[(pyridine-2-ylmethylene)amino]phenol} containing one pyridine ring and one phenolic ring, from which the dichloro-bridged copper dimer $[\text{CuLCl}]_2$ is obtained. The complex provides unique trigonal-bipyramidal geometry and exhibits unusual ferromagnetic interaction.

Results and Discussion

UV Spectra

The UV-visible spectroscopic data for the ligand and the complex were studied in MeOH. HL exhibits three maxima centered at 289, 361, and 442 nm while $[\text{CuLCl}]_2$ shows three maxima at 281, 357, and 506 nm. The absorption bands at 200–400 nm in $[\text{CuLCl}]_2$ may correspond to the ligand-centered π - π^* transitions, and the band at 506 nm may correspond to the ligand-to-metal charge transfer transition. The shifts and the new absorptions may account for the coordination.

Description of Structure

The crystal structure of $[\text{CuLCl}]_2$ is shown in Figure 1. Selected bond lengths and bond angles are listed in Table 1. Besides Cl[−] bridges, the coordination sites of Cu^{II} are the N_{imine}, N_{py}, and the deprotonated phenolate oxygen O_{pheno} from the Schiff-base ligand. The distortion parameter τ ^[4] of 0.448 (near to 0.50) in $[\text{CuLCl}]_2$ indicates that the geometry may be described as either a distorted square-pyramid

[a] College of Chemistry, Beijing Normal University, Beijing 100875, China
Fax: +86-10-64463640
E-mail: qicmin@sohu.com
mashulan@263.net

[b] State Key Laboratory of Rare Earth Materials Chemistry and Application, College of Chemistry and Molecular Engineering, Peking University, Beijing 100871, China

Supporting information for this article is available on the WWW under <http://www.eurjic.org> or from the author.

(SP) or a trigonal-bipyramid (TBP), which resembles other dimers (τ is 0.487, 0.485, and 0.455, respectively).^[3b,5] In the TBP geometry for $[\text{CuLCl}]_2$, the apical sites are occupied by O1 and N2, with Cl1, Cl1A, and N1 making up the equatorial plane. The Cu^{II} ion sits 0.043 Å apart from the plane, and the apical O1 and N2 are located −1.954 and 1.955 Å on either side. If the geometry is viewed as a SP, the axial ligand is Cl1A and the basal ones consist of N1, N2, O1, and Cl1, with Cu^{II} sitting 0.455 Å from the plane. The bond angles for two idealized five-coordinate geometries are listed in Table 1. The distortion from ideal TBP geometry is observed in equatorial bond angles of 90.77, 132.34, and 136.77°, showing deviation from ideal 120° angles. The distortion from an ideal SP is much more obvious in the angles of 136.77° for N1–Cu1–Cl1 and 132.34° for N1–Cu1–Cl1A, showing significant deviation from the ideal angles of 180 and 90°, respectively. So this system is much more readily described as a distorted TBP. The bridging Cu_2Cl_2 unit is constrained to be planar by the presence of the crystallo-

graphic center. The Cu–Cl–Cu angle of 89.23° is slightly shorter than the average 89.40° and the Cu–Cu distance of 3.424 Å is in agreement with the average value for 188 chloro-bridged copper(II) dimers (3.499 Å) in CSD. The two Cu–Cl bridging distances of 2.444 and 2.430 Å fall into the range between 2.309 Å (short)^[6] and 2.554 Å (long)^[7] for five-coordinate copper(II) complexes.

Magnetic Properties

Variable temperature magnetic susceptibility on $[\text{CuLCl}]_2$ was measured in the range 2.0–300 K (Figure 2). At room temperature $\chi_{\text{m}}T$ is 0.88 cm³ mol^{−1} K, which is slightly higher than the expected value 0.75 cm³ mol^{−1} K for two uncoupled spin-only Cu^{II} ions ($S = 1/2$, $g = 2$). Upon cooling from room temperature, $\chi_{\text{m}}T$ increases very smoothly increasing continuously below 20 K, and reaching a value of 0.99 cm³ mol^{−1} K near to 2.0 K. The χ_{m}^{-1} vs. T plot is essentially linear, and least-squares fitting of the data to the Curie–Weiss law gave $C = 0.88$ cm³ mol^{−1} K and $\theta = +0.52$ K. The increase of $\chi_{\text{m}}T$ upon cooling, and the small positive Weiss constant indicates that there exists a weak but unquestionably ferromagnetic coupling between two Cu^{II} ions. The magnetization measured at 2.00 K increases with the field, and reaches 2.02 $N\beta$ per Cu_2 at 50 kOe, slightly higher than the expected saturation value of 2 $N\beta$ for two spin-only Cu^{II} ions with $S = 1/2$, $g = 2.0$. The expression of the molar susceptibility χ_{m} is presented by the following Bleaney–Bowers equation:

$$\chi_{\text{m}} = 2Ng^2\beta^2/kT \cdot [3 + \exp(-2J/kT)]^{-1}$$

The best fitting for the experiment data leads to the parameters $g = 2.17$ and $2J = 1.52$ cm^{−1}. The agreement factor R , defined as $\sum(\chi_{\text{m}}T_{\text{obs}} - \chi_{\text{m}}T_{\text{calc}})^2 / \sum(\chi_{\text{m}}T_{\text{obs}})^2$, is equal to $4.26 \cdot 10^{-4}$. The solid line in Figure 2 corresponds to the best theoretical fit.

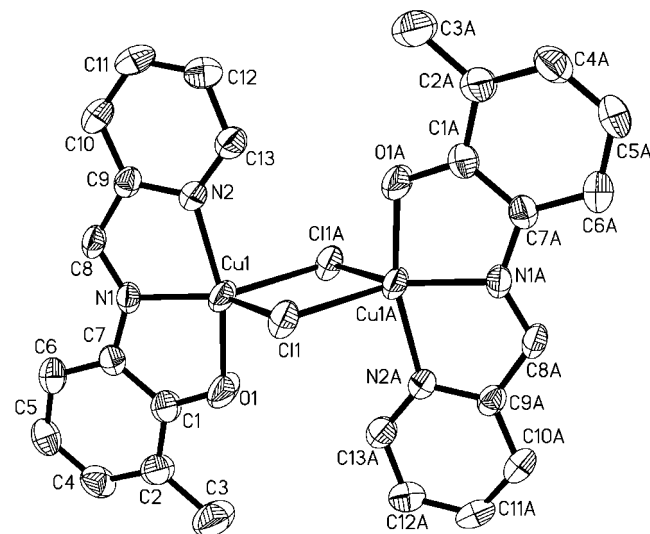


Figure 1. Molecular structure of the complex $[\text{CuLCl}]_2$ (thermal ellipsoids at 30% probability).

Table 1. Important bond lengths and angles for $[\text{CuLCl}]_2$ and corresponding angles for two idealized geometries.

Atoms	Distance [Å]	Atoms	Angle [°]	TBP ^[b] [°]	SP ^[c] [°]
Cu1–O1	1.929(3)	O1–Cu1–N1	83.48(11)	90	90
Cu1–N1	1.961(3)	O1–Cu1–N2	163.66(11)	180	180
Cu1–N2	2.021(3)	O1–Cu1–Cl1	96.10(11)	90	90
Cu1–Cl1	2.4444(11)	O1–Cu1–Cl1A	96.85(12)	90	90
Cu1–Cl1A ^[a]	2.4302(11)	N1–Cu1–N2	80.18(12)	90	90
Cu1–Cu1A	3.424	N1–Cu1–Cl1	136.77(9)	120	180
Cl1–O1	1.313(4)	N1–Cu1–Cl1A	132.34(9)	120	90
C7–N1	1.396(4)	N2–Cu1–Cl1	95.97(9)	90	90
C8–N1	1.282(4)	N2–Cu1–Cl1A	93.95(9)	90	90
C9–N2	1.352(4)	Cl1–Cu1–Cl1A	90.77(3)	120	90

[a] Symmetry transformations used to generate equivalent atoms: #1 $-x + 1, -y, -z + 1$. [b] Angle for TBP geometry at Cu, with O1 and N2 axial and N1, Cl1 and Cl1A equatorial. [c] Angle for SP geometry at Cu, with Cl1A axial and O1, N1, N2 and Cl1 equatorial.

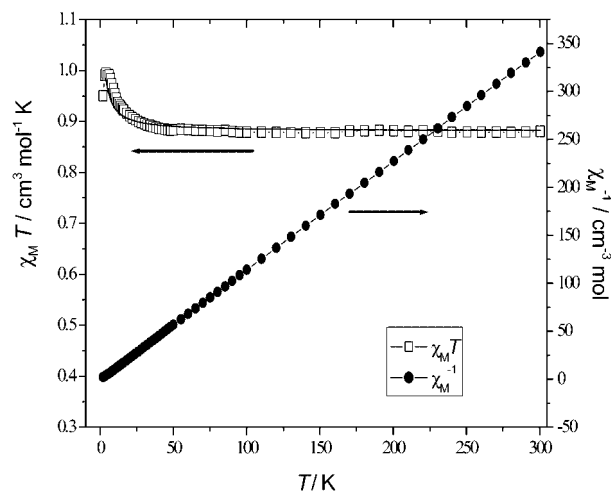
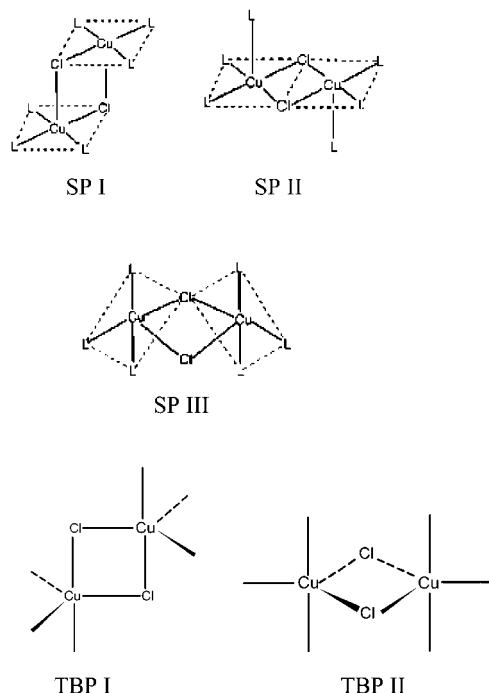


Figure 2. The plot of temperature dependence of χ_{m}^{-1} (●) and $\chi_{\text{m}}T$ (□) of complex $[\text{CuLCl}]_2$ measured at 1000 Oe. The solid line represents the best fit of the experimental data as discussed in the text.

The sign and magnitude of the coupling constant $2J$ for pentacoordinate $\text{Cu}(\mu\text{-Cl})_2\text{Cu}$ dimers depend mainly on the $\text{Cu}\text{--}\text{Cl}\text{--}\text{Cu}$ bridging angle φ , the $\text{Cu}\text{--}\text{Cl}$ distance, the nature of the terminal ligands, and the distortions of the coordination geometry.^[8] The SP geometry for these dimers is the usual one, but a distortion toward TBP can exist. Three different SP geometries have been experimentally characterized: square pyramids sharing a base-to-apex edge with parallel basal planes (SP I), square pyramids sharing a basal edge with coplanar basal planes (SP II), and square pyramids that also share a base-to-apex edge, but with perpendicular basal planes (SP III). For the less common TBP geometry, two types are formed: TBP I is formed by sharing an edge joining the axial and equatorial chloride atoms (axial-equatorial dimer) while TBP II is formed by sharing an edge joining two equatorial chloride ligands (equatorial-equatorial dimer). For reason of contrast, the SP I,^[3c,9] SP II,^[10] SP III^[3d] compounds with ferromagnetic coupling, and the TBP I^[3a,3b,5,11] and TBP II^[12] compounds known so far with ferromagnetic or antiferromagnetic coupling, are listed in Table 2. The SP I compounds usually show small ferromagnetic^[3c,9] or antiferromagnetic coupling constants,^[13] and those of SP II show antiferromagnetic behavior when halide ions are present in the terminal ligands^[14] and ferromagnetic behavior in the presence of N-donors.^[10] The only SP III compound known so far presents ferromagnetic coupling ($2J = +85.88 \text{ cm}^{-1}$).^[3d] The TBP I compounds usually exhibit antiferromagnetic behavior^[3a,3b,5b,11] while TBP II compounds (only two examples) often show ferromagnetic behavior.^[12]



The values of $\text{Cu}\text{--}\text{Cl}\text{--}\text{Cu}$ angle φ in TBP I complexes are always obtuse and as shown in Table 2 (structures **10–15**) are close to 95° (from 94.8 to 97.9°). While the φ values in TBP II geometries are always lower than 90° , and for the two compounds **16** and **17** they are in the range $81.8\text{--}89.3^\circ$.^[12] The $2J$ obtained from the TBP complexes in

Table 2. The structural and magnetic properties for some $\text{Cu}(\mu\text{-Cl})_2\text{Cu}$ dimers.^[a]

Complexes	$\text{Cu}\text{--}\text{Cu}'$ [Å]	$\text{Cu}\text{--}\text{Cl}$ R [Å]	$\text{Cu}\text{--}\text{Cl}\text{--}\text{Cu}'$ φ [°]	φ/R [°/Å]	$2J$ [cm^{-1}]	Geom.	Ref.
1. $[\text{Cu}(\text{dmgH})\text{Cl}_2]_2$	3.445	2.698	88.0	32.62	+0.62 (Y) ^[b]	SP I	[9a]
2. $[\text{Cu}(\text{pfsa})\text{Cl}]_2$	3.825	2.846	95.27	33.6	+0.30 (Y)	SP I	[3c]
3. $[\text{Cu}(\text{pmda})\text{Cl}]_2(\text{ClO}_4)_2$	3.396	2.581	88.2	34.17	+2.24 (Y)	SP I	[9b]
4. $[\text{Cu}(\text{iyda})\text{Cl}]_2(\text{ClO}_4)_2$	3.494	2.657	88.81	33.42	+1.16 (Y)	SP I	[9c]
5. $[\text{Cu}(\text{bpdio})\text{Cl}_2]_2$	3.842	2.844	96.68	33.99	+4.87 (Y)	SP I	[9d]
6. $[\text{Cu}_2(\text{baamo})_2\text{Cl}_2]$	3.418	2.808	82.9	29.52	+12.0 (N) ^[b]	SP I	[9e]
7. $[\text{CuCl}_2(\text{pytn})]_2$	3.612	2.906	88.60	30.49	+27.46 (N)	SP I	[9f]
8. $[\text{CuCl}(\text{hpba})_3]_2$	3.394	2.316	94.51	40.81	+33.70 (N)	SP II	[10]
9. $[\text{Cu}_2(\text{dpt})_2\text{Cl}_2](\text{Cl})_2$	3.551	2.545	91.4	35.91	+85.88 (N)	SP III	[3d]
10. $[\text{Cu}(\text{Et}_3\text{en})\text{Cl}_2]_2$	3.703	2.728	94.84	34.75	+0.10 (Y)	TBP I	[3b]
11. $[\text{Cu}(\text{ampy})\text{Cl}_3]_2$	—	2.330	94.9	40.73	+42.0 (N)	TBP I	[5a]
12. $[\text{Co}(\text{en})_3]_2[\text{CuCl}_8]\text{Cl}_2$	3.722	2.703	95.2	35.22	−14.60 (Y)	TBP I	[5b,11a]
13. $[\text{Cu}(\text{dmtcp})\text{Cl}_2]_2$	3.570	2.543	95.34	37.49	−38.80 (Y)	TBP I	[11b]
14. $[\text{Cu}(\text{guaH})\text{Cl}_3]_2$	3.575	2.447	97.9	40.01	−82.6 (Y)	TBP I	[3a,11c]
15. $[\text{Cu}(4\text{-Metz})(\text{DMF})\text{Cl}_2]_2$	3.721	2.724	95.3	34.99	−3.60 (Y)	TBP I	[3b]
16. $[\text{Cu}(\text{btaH})_2\text{Cl}_2]_2 \cdot \text{H}_2\text{O}$	3.520	2.694	89.3	33.77	+1.80 (Y)	TBP II	[12a,12b]
	3.448	2.544	87.5	(mean)			
17. $[\text{Cu}_2\text{Cl}_3(\text{bmdz})_3]\text{Cl} \cdot 4\text{H}_2\text{O}$	3.386	2.424	89.1	33.90	+5.60 (Y)	TBP II	[12c]
		2.620	81.8	(mean)			
$[\text{CuLCl}]_2$	3.424	2.444	89.23	36.51	+1.52 (N)	TBP II	this work

[a] Abbreviations: dmgh, dimethylglyoxime; pfsa, 3-[*N*-2-(pyridylethyl)formimidoyl]salicylic acid; pmda, 1-(2-pyridylmethyl)-1,5-diazacyclooctane; iyda, 1-(imidazol-4-ylmethyl)-1,5-diazacyclooctane; bpdio, 2,2-bis(2-pyridyl)-1,3-dioxolane; baamo, 8-amino-5-aza-4-methyl-3-octene-2-onate; pytn, 2-(pyrazol-1-yl)-2-thiazoline; hpba, hydrotris(1-pyrazolyl)borate anion; dpt, dipropylentriamine; Et_3en , *N,N,N'*-triethylenediamine; ampy, 3-aminopyridinium; en, ethylenediamine; dmtcp, 3,5-dimethyl-1-thiocarboxamide pyrazole; guaH, guaninium; 4-Metz, 4-methylthiazole, DMF, *N,N*-dimethylformamide; btaH, benzotriazole; bmdz, benzimidazole; HL, 2-methyl-6-[(pyridine-2-ylmethylene)amino]phenol. [b] Y or N: obey or does not obey the empirical correlation between $2J$ and φ/R described by Hatfield.

Table 2 including our present $[\text{CuLCl}]_2$ are consistent with the 90° angle rule^[15] that the coupling is ferromagnetic for the φ value near to 90° and antiferromagnetic for that diverging from 90° . The φ values of 89.3 and 89.1° in **16** and **17**^[12] and 89.23° in the present work are fairly close to 90° , and that induces their ferromagnetic coupling ($2J > 0$). TBP I compounds **12–15** have φ values with a larger divergence from 90° , and hence antiferromagnetic interactions occur ($2J < 0$). Because the ferromagnetic coupling may increase when the Cu–Cl bridging distance decreases,^[8b] the stronger ferromagnetic interaction in **11** may be thanks to its shorter Cu–Cl bridging bonds (2.330 \AA) though with a large φ value (94.9°). Another compound, $[(\text{terpy})\text{CuCl}]_2\text{[PF}_6\text{]}_2$, has a φ value near to 90° (89.9°)^[13a] but shows antiferromagnetic coupling ($2J = -2.32 \text{ cm}^{-1}$). The longer Cu–Cl bridging distance of 2.72 \AA and the SP geometry may induce its antiferromagnetic behavior.

The bridge angle can determine the sign of the exchange-coupling constant, and the bond length in the superexchange pathway may deflect the magnitude of $2J$. Hatfield and co-workers have proposed an empirical correlation between $2J$ and the φ/R_0 ratio in $\text{Cu}(\mu\text{-Cl})_2\text{Cu}$ complexes,^[3b,16] where R_0 is the (longer) axial Cu–Cl bridging distance in the SP geometry while representing the equatorial distance in the TBP geometry.^[3b] They found that for a value of φ/R_0 lower than 32.6 or higher than $34.8 [^\circ/\text{\AA}]$ the exchange interaction is antiferromagnetic and for values falling between these limits the interactions are ferromagnetic. Their analysis was predominantly for the SP I and TBP I systems involving the axial-equatorial dimers.^[3b] From Table 2 we can see that most of the compounds with SP I and TBP I geometries are consistent with this correlation. The structures of TBP II complexes **16** and **17** are complicated by the presence of two crystallographically independent dimers in **16** and two nonequivalent Cu–Cl–Cu bridges in **17**, so we can only use the mean φ/R_0 ratios (33.77 for **16** and 33.90 for **17**). According to the mean φ/R_0 ratios, their magnetic coupling also fits the prediction of the correlation between $2J$ and φ/R_0 . Our present complex $[\text{CuLCl}]_2$ has a relative simple and sterling structure and has an φ/R_0 value of 36.50 , and it shows ferromagnetic coupling, which does not fit the trend of Hatfield's analysis. This may result from

its unique geometry distortion. We can not substantiate the magneto-structural correlation due to the very sparse number of examples of this kind of TBP II complexes.

The unpaired spin should lie predominantly in the $d_{x^2-y^2}$ orbital in the SP geometry, and in the d_{z^2} orbital in the TBP geometry.^[3b,12c,17] But for the axial-equatorial SP I and TBP I dimers, this distinction is unnecessary, since they are interconvertible by a single angular deformation. Thus, they may be viewed as belonging to the same structural type and their magnetic properties can be compared directly as in the correlation between $2J$ and φ/R_0 by Hatfield.^[3b] This statement is restricted to SP I and TBP I complexes, since the deformation would not transform SP I to the equatorial-equatorial TBP II dimer. An extended Hückel molecular orbital calculation for the TBP II compound **17** revealed that its occupied molecular orbitals were located mainly in the d_{z^2} orbitals.^[12c] Therefore, the relative orientation of the metallic part of the magnetic orbitals of our present complex may be represented as depicted in Figure 3. The distortion from SP to TBP induced a change in the d_{Cu} metal orbital from $d_{x^2-y^2}$ to d_{z^2} , and an effective overlap occurs between two Cu centers, leading to the increase of the ferromagnetic contribution for $[\text{CuLCl}]_2$.^[3a,8a,13a]

Another interesting structural feature for $[\text{CuLCl}]_2$ is that its Cu_2Cl_2 bridging unit is nearly a square (the two Cu–Cl bridging bonds are 2.444 and 2.430 \AA , and the Cu–Cl–Cu' and Cl–Cu–Cl' angles are 89.23 and 90.77° , respectively), which is not observed in other known $\text{Cu}(\mu\text{-Cl})_2\text{Cu}$ complexes. There are three complexes containing near Cu–Cl bridging bonds: $[\text{KCuCl}_3]_2$ (2.314 , 2.322 \AA)^[18] $[(i\text{PrNH}_3)(\text{CuCl}_3)]_2$ (2.301 , 2.315 \AA)^[14b] and $[\text{CuCl}(\text{hpba}_3)]_2$ (2.306 , 2.316 \AA)^[10] But they all adopt the SP II geometries, have bridging angles diverging considerably from 90° (95.9 , 95.4 , and 94.51°), and exhibit divergent magnetic interaction ($2J = -38.23$, -19.46 , and $+33.7 \text{ cm}^{-1}$, respectively). When $2J$ values of these complexes were plotted against φ , the points fell nearly in a straight line of slope $-48.6 [\text{cm}^{-1}/^\circ]$ and passed through $2J = 0$ at 95.1° .^[8a,10] $[\text{CuLCl}]_2$ is not placed close to the line, which may be due to its unique TBP geometry.

Many chloro-bridged Cu^{II} dimers use Cl^- as terminal ligands, and a change from antiferromagnetic to ferromag-

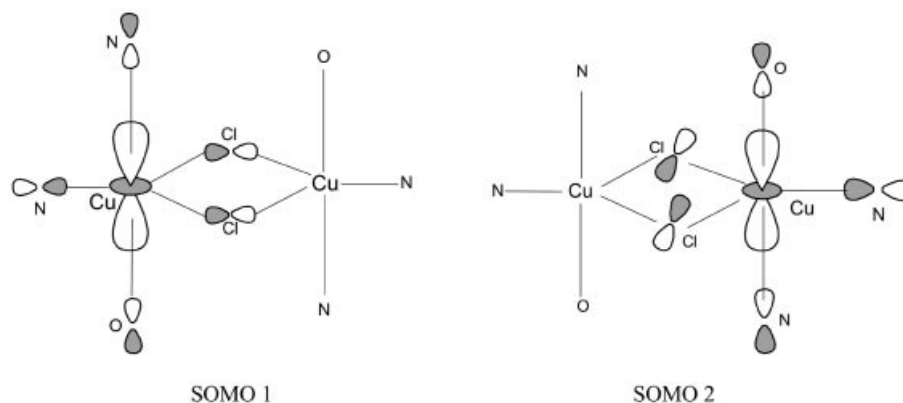


Figure 3. The two SOMOs of the complex $[\text{CuLCl}]_2$.

netic behavior may occur when Cl^- is substituted by a N donor.^[8b] Our present complex $[\text{CuLCl}]_2$ and **2**^[3c] are two unique cases containing phenolate oxygen donors. The deprotonation of the phenolate group can provide one anion and cut down the number of Cl^- anions thus featuring the unprecedented magnetic behavior.

$[\text{CuLCl}]_2$ represents a very rare example of the unique equatorial-equatorial TBP geometry. Its interesting structure and the novel ferromagnetic behavior might provide useful information for the magneto-structural correlations for this TBP system in the future. With continued research efforts designed to improve theoretical models and to obtain a greater number of experimental examples, the nature of the relationship between the structural properties and the exchange-coupling constant for TBP systems can be refined.

Conclusions

In summary, we have prepared and characterized a novel equatorial-equatorial trigonal bipyramidal copper dimer with ferromagnetic exchange interaction. The complex has a Cu–Cl–Cu bridging angle close to 90° and two shorter and near Cu–Cl bridging bonds, and the deprotonation of the phenolate group can reduce the number of Cl^- anions. The distortion from SP to TBP geometry may cause an effective overlap between two Cu centers. All these features of the complex may thus increase its ferromagnetic behavior.

Experimental Section

General Remarks: All commercially available chemicals were of analytical grade and were used as received. C, H, and N were determined with an Elementar vario EL elemental analyzer. UV/Vis spectra were measured with a GBC Cintra 10e UV/Vis spectrophotometer in MeOH solution. The IR spectra were recorded with a Nicolet-AVATAR 360 FT-IR spectrometer using KBr pellets in the $4000\text{--}400\text{ cm}^{-1}$ regions. ^1H NMR spectra were recorded with a Varian 500 Bruker spectrometer in DMSO. Variable-temperature magnetic susceptibility data for the crystalline sample were obtained in an external field of 1000 G on an Oxford Maglab 2000 system magnetometer in the $2\text{--}300\text{ K}$ temperature range. The susceptibilities were corrected for diamagnetism with Pascal's constants for all the constituent atoms.

Synthesis of HL: A mixture of pyridine-2-carbaldehyde (0.107 g, 1 mmol) and 2-amino-6-methylphenol (0.123 g, 1 mmol) was refluxed in anhydrous ethanolic solution (20 mL) for 2 h. After the solvent was removed, *n*-hexane was added (20 mL) and the mixture was refluxed for another 0.5 h. The reaction mixture was filtered and left to stand at room temperature and then brown crystals were obtained from the filtrate after 15 min. Yield: 0.172 g, 81%. M. p. $95\text{--}96^\circ\text{C}$. $\text{C}_{13}\text{H}_{12}\text{N}_2\text{O}$ ($M_r = 212.10$): calcd. C 73.56, H 5.70, N 13.20; found C 73.57, H 5.92, N 13.22. ^1H NMR (500 MHz, DMSO): $\delta = 8.76$ (s, 1 H, phenol-OH), 8.74 (s, 1 H, imide-H), 8.70 (d, $J = 4.2\text{ Hz}$, 1 H, pyridine-H), 8.58 (d, $J = 7.9\text{ Hz}$, 1 H, pyridine-H), 7.96 (t, $J = 7.6\text{ Hz}$, 1 H, pyridine-H), 7.50 (t, $J = 6.3\text{ Hz}$, 1 H, pyridine-H), 7.28 (d, $J = 7.9\text{ Hz}$, 1 H, Ar-H), 7.08 (d, $J = 7.3\text{ Hz}$, 1 H, Ar-H), 6.78 (t, $J = 7.7\text{ Hz}$, 1 H, Ar-H), 2.22 (s, 3 H, $-\text{CH}_3$) ppm. IR (KBr pellet): $\tilde{\nu} = 3402, 3061, 2918, 1627, 1600,$

1582, 1566, 1476, 1433, 1344, 1235, 1205, 1163, 1079, 1013, 944, 834, 783, 742, 733, 598 cm^{-1} . UV/Vis (λ_{max} , MeOH): 289, 361, 442 nm.

Synthesis of Complex $[\text{CuLCl}]_2$: To a 10-mL $\text{CH}_2\text{Cl}_2\text{--CH}_3\text{OH}$ (1:1) yellow solution of HL (0.011 g, 0.05 mmol), a 5-mL CH_3OH solution of $\text{CuCl}_2\cdot 2\text{H}_2\text{O}$ (0.008 g, 0.05 mmol) was added dropwise with continuous stirring, and then the mixture was refluxed for 1 h. The reaction mixture was filtered and left to stand at room temperature. On slow evaporation of the solution for several days, the deep red crystals of $[\text{CuLCl}]_2$ suitable for X-ray analysis were collected. $\text{C}_{13}\text{H}_{11}\text{ClCuN}_2\text{O}$ ($M_r = 310.23$): calcd. C 50.33, H 3.55, N 9.02; found C 50.43, H 3.45, N 9.27. IR (KBr pellet): $\tilde{\nu} = 3410, 3056, 3002, 1605, 1593, 1543, 1477, 1449, 1423, 1359, 1276, 1247, 1205, 1157, 1075, 922, 848, 782, 746\text{ cm}^{-1}$. UV/Vis (λ_{max} , MeOH): 281, 357, 506 nm.

X-ray Crystallographic Study: The crystal with dimensions $0.30 \times 0.22 \times 0.10\text{ mm}$ was selected for X-ray diffraction experiments. The measurements were performed with a Bruker SMART 1000 CCD diffractometer at room temperature (293 K) with graphite monochromatized Mo- K_α radiation ($\lambda = 0.71073\text{ \AA}$). Semi-empirical absorption corrections were applied using the SADABS program. The structures were solved by direct methods and refined by full-matrix least-squares on F^2 using the SHELXS-97 and SHELXL-97 programs.^[19] All non-hydrogen atoms were refined with anisotropic displacement parameters and the hydrogen atoms were generated geometrically and treated by a mixture of independent and constrained refinements. A summary of the crystallographic data and details of the structure refinements are listed in Table 3. CCDC-285069 contains the supplementary crystallographic data for this paper. These data can be obtained free of charge from The Cambridge Crystallographic Data Centre via www.ccdc.cam.ac.uk/data_request/cif.

Table 3. Crystal data and structure refinement details for complex $[\text{CuLCl}]_2$.

Empirical formula	$\text{C}_{26}\text{H}_{22}\text{Cl}_2\text{Cu}_2\text{N}_4\text{O}_2$
Formula weight	620.46
Temperature [K]	294(2)
Wavelength [\AA]	0.71073
Crystal system	orthorhombic
Space group	<i>Pbca</i>
Unit cell dimensions	$a = 14.807(3)\text{ \AA}$, $a = 90^\circ$ $b = 8.8132(16)\text{ \AA}$, $\beta = 90^\circ$ $c = 18.846(3)\text{ \AA}$, $\gamma = 90^\circ$
Volume [\AA^3]	2459.4(8)
Z , calculated density [g/cm^3]	8, 1.676
Absorption coefficient [mm^{-1}]	1.980
$F(000)$	1256
Crystal size [mm]	$0.30 \times 0.22 \times 0.10$
θ range for data collection	$2.16\text{--}26.47^\circ$
Reflections collected / unique	12883 / 2524 [$R_{\text{int}} = 0.0599$]
Data / restraints / parameters	5444 / 39 / 381
Goodness of fit on F^2	1.003
Final R indices [$I > 2\sigma(I)$]	$R_1 = 0.0412$, $wR_2 = 0.0944$
R indices (all data)	$R_1 = 0.0700$, $wR_2 = 0.1114$

Acknowledgments

This work was supported by the National Natural Science Foundation of China (No. 20371009) and Key Laboratory of Radiopharmaceuticals of Beijing Normal University, Ministry of Education.

- [1] a) J. S. Miller, A. J. Epstein, *Angew. Chem. Int. Ed. Engl.* **1994**, *33*, 385–415; b) J. S. Miller, A. J. Epstein, W. M. Reiff, *Science* **1988**, *240*, 40–47.
- [2] a) P. J. Hay, J. C. Thibeault, R. Hoffmann, *J. Am. Chem. Soc.* **1975**, *97*, 4884–4899; b) V. H. Crawford, H. W. Richardson, J. R. Wasson, D. J. Hodgson, W. E. Hatfield, *Inorg. Chem.* **1976**, *15*, 2107–2110; c) M. F. Charlot, O. Kahn, S. Jeannin, Y. Jeannin, *Inorg. Chem.* **1980**, *19*, 1410–1411.
- [3] a) R. F. Drake, V. H. Crawford, N. W. Laney, W. E. Hatfield, *Inorg. Chem.* **1974**, *13*, 1246–1250; b) W. E. Marsh, K. C. Patel, W. E. Hatfield, D. J. Hodgson, *Inorg. Chem.* **1983**, *22*, 511–515; c) F. Tuna, L. Patron, Y. Journaux, M. Andruh, W. Plass, J.-C. Trombe, *J. Chem. Soc., Dalton Trans.* **1999**, 539–545; d) M. Rodríguez, A. Llobet, M. Corbella, A. E. Martell, J. Reibenspies, *Inorg. Chem.* **1999**, *38*, 2328–2334.
- [4] A. W. Addison, T. N. Rao, J. Reedijk, J. van Rijn, G. C. Verschoor, *J. Chem. Soc., Dalton Trans.* **1984**, 1349–1356.
- [5] a) J. T. Blanchette, R. D. Willett, *Inorg. Chem.* **1988**, *27*, 843–849; b) D. J. Hodgson, P. K. Hale, W. E. Hatfield, *Inorg. Chem.* **1971**, *10*, 1061–1067.
- [6] I. J. Bruno, J. C. Cole, P. R. Edgington, M. Kessler, C. F. Macrae, P. McCabe, J. Pearson, R. Taylor, *Acta Crystallogr., Sect. B* **2002**, *58*, 389–397.
- [7] A. G. Orpen, L. Brammer, F. H. Allen, O. Kennard, D. G. Watson, R. Taylor, *J. Chem. Soc., Dalton Trans.* **1989**, 1–83.
- [8] a) M. Rodríguez, A. Llobet, M. Corbella, *Polyhedron* **2000**, *19*, 2483–2491; b) A. Rodríguez-Fortea, P. Alemany, S. Alvarez, E. Ruis, *Inorg. Chem.* **2002**, *41*, 3769–3778.
- [9] a) M. Mègnamisi-Bélombé, M. A. Novotny, *Inorg. Chem.* **1980**, *19*, 2470–2473; b) X.-H. Bu, M. Du, Z.-L. Shang, L. Zhang, Q.-H. Zhao, R.-H. Zhang, M. Shionoya, *Eur. J. Inorg. Chem.* **2001**, 1551–1558; c) X.-H. Bu, M. Du, L. Zhang, Z.-L. Shang, R.-H. Zhang, M. Shionoya, *J. Chem. Soc., Dalton Trans.* **2001**, 729–735; d) C. J. O'Connor, *Inorg. Chim. Acta* **1987**, *127*, 29–30; e) E. Kwiatkowski, M. Kwiatkowski, A. Olechnowicz, J. Mrozinski, D. M. Ho, E. Deutsch, *Inorg. Chim. Acta* **1989**, *158*, 37–42; f) A. Bernalte-García, A. M. Lozano-Vila, F. Luna-Giles, R. Pedrero-Marín, *Polyhedron* **2006**, *25*, 1399–1407.
- [10] S. G. N. Roundhill, D. M. Roundhill, D. R. Bloomquist, C. Landee, R. D. Willett, D. M. Dooley, H. B. Gray, *Inorg. Chem.* **1979**, *18*, 831–835.
- [11] a) K. T. McGregor, D. B. Losee, D. J. Hodgson, W. E. Hatfield, *Inorg. Chem.* **1974**, *13*, 756–759; b) I. R. Evans, J. A. K. Howard, L. E. M. Howard, J. S. O. Evans, Ž. K. Jaćimović, V. S. Jevtović, V. M. Leovac, *Inorg. Chim. Acta* **2004**, *357*, 4528–4536; c) J. A. Carrabirie, M. Sundaralingam, *J. Am. Chem. Soc.* **1970**, *92*, 369–371.
- [12] a) I. Søjtofte, K. Nielsen, *Acta Chem. Scand. Ser. A* **1981**, *A35*, 733–738; b) D. J. Hodgson, E. Pedersen, *Acta Chem. Scand. Ser. A* **1982**, *A36*, 281–282; c) A. Tosik, W. Maniukiewicz, M. Bukowska-Strzyewska, J. Mrozinski, M. P. Sigalas, C. A. Tsipis, *Inorg. Chim. Acta* **1991**, *190*, 193–203.
- [13] a) T. Rojo, M. I. Arriortua, J. Ruiz, J. Darriet, G. Villeneuve, D. Beltranporter, *J. Chem. Soc., Dalton Trans.* **1987**, 285–291; b) S. C. Lee, R. H. Holm, *Inorg. Chem.* **1993**, *32*, 4745–4753.
- [14] a) C. P. Landee, A. Djili, D. F. Mudgett, M. Newhall, H. Place, B. Scott, R. D. Willett, *Inorg. Chem.* **1988**, *27*, 620–627; b) S. A. Roberts, D. R. Bloomquist, R. D. Willett, H. W. Dodgen, *J. Am. Chem. Soc.* **1981**, *103*, 2603–2610.
- [15] a) P. J. Hay, J. C. Thibeault, R. Hoffmann, *J. Am. Chem. Soc.* **1975**, *97*, 4884–4899; b) J. B. Goodenough, *Phys. Rev.* **1955**, *100*, 564–573.
- [16] W. E. Marsh, W. E. Hatfield, D. J. Hodgson, *Inorg. Chem.* **1982**, *21*, 2679–2684.
- [17] A. Benzekri, P. Dubourdeaux, J.-M. Latour, J. Laugier, P. Rey, *Inorg. Chem.* **1988**, *27*, 3710–3716.
- [18] R. D. Willett, C. Dwiggs Jr, R. F. Kruh, R. E. Rundle, *J. Chem. Phys.* **1963**, *38*, 2429–2436.
- [19] G. M. Sheldrick, *SHELXS-97* and *SHELXL-97*, programs for the solution and refinement of crystal structures, University of Göttingen, Göttingen, Germany, **1997**.

Received: September 23, 2006
Published Online: January 8, 2007